Electronic Supplementary Material (ESI) for RSC Advances.

Drug and dye binding induced folding of the intrinsically disordered antimicrobial peptide CM15

Ferenc Zsila,* Szilvia Bősze, Kata Horváti, Imola Cs. Szigyártó, Tamás Beke-Somfai

Electronic Supplementary Information

Peptide synthesis and purification

CM15 was produced on solid phase (Fmoc-Rink Amide MBHA, capacity = 0.67 mmol/g) resin in an automated peptide synthesizer (Syro-I, Biotage) using standard Fmoc/^{t}Bu strategy with DIC/HOBt coupling reagents. Peptide was cleaved from the resin with TFA/H_2O/TIS (9.5 : 2.5 : 2.5 v/v) mixture (2 hrs, RT). After filtration the compound was precipitated in cold diethyl ether, centrifuged (4000 rpm, 5 min) and freeze-dried from water. Crude product was purified by RP-HPLC on a semipreparative C-18 Phenomenex Jupiter column (250 × 10 mm) using gradient elution, consisted of 0.1% TFA in water (eluent A) and 0.1% TFA in acetonitrile/water = 80/20 (v/v) (eluent B).

Peptide characterization

Purified CM15 was analysed by RP-HPLC on an analytical C-18 Zorbax (150 × 4.4 mm) column using gradient elution with the above mentioned eluent A and B (flow rate was 1 mL/min, gradient was 5-100 B%, 20 min, UV detection at 220 nm).

Molecular mass of the peptide was determined by using a Bruker Esquire 3000+ ESI mass spectrometer. Peptide samples were dissolved in a mixture of acetonitrile/water = 1/1 (v/v) containing 0.1% acetic acid and introduced by a syringe pump with a flow rate of 10 μL/min. The peptide content was determined by amino acid analysis using a Sykam Amino Acid S433H analyser equipped with an ion-exchange separation column and postcolumn derivatization. Prior to analysis, samples were hydrolysed with 6 M HCl in sealed and evacuated tubes at 110 °C for 24 h. For post-column derivatization the ninhydrin-method was used.

peptide	*sequence*	Z^a	$M_{av}{}^b$ *calcd/found*	$R_t{}^c$ *(min)*	*peptide content* ^{e} *%*
CM15	KWKLFKKIGAVLKVL	+6	1770.3/1770.4	13.6	52

C-terminus of the peptides was amidated.

[a] *Z*: net charge at neutral pH. Calculated by the number of (K+R)-(E+D). Positive charge at the *N*-terminus increases *Z* by 1 unit.

[b] Measured average molecular mass by Bruker Esquire 3000+ ESI-MS.

[c] Analytical RP-HPLC, gradient: 5% B, 5 min.; 5-100% B, 20 min.

[d] Peptide content was determined by amino acid analysis using freeze-dried final product.

Analytical HPLC chromatogram:

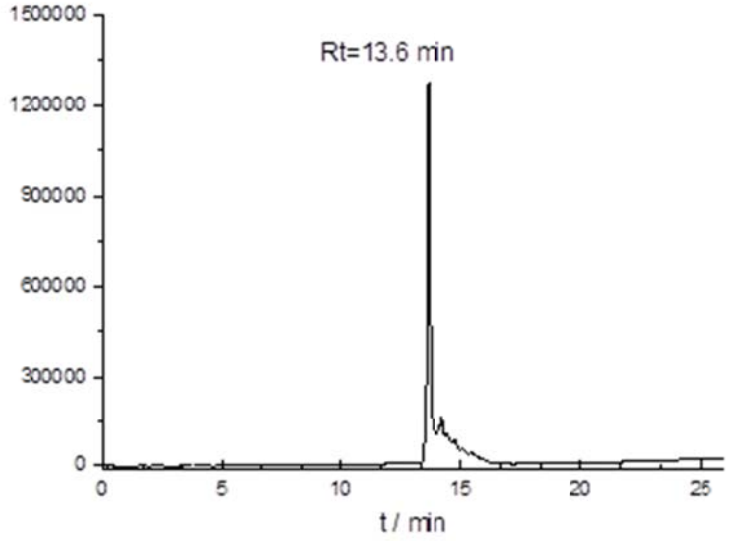

Mass spectrum:

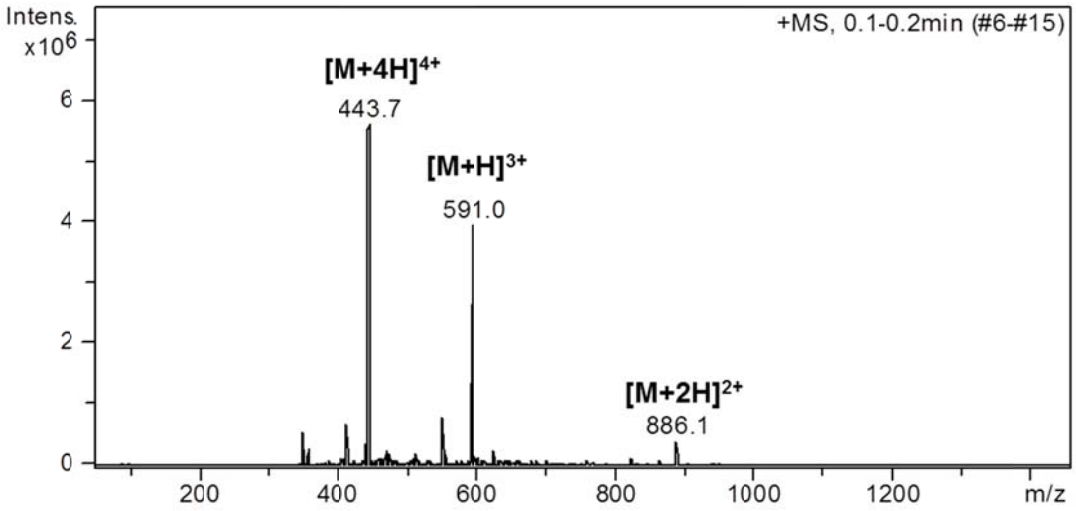

Computational details

To support the experimental investigations with a molecular level insight into the potential interactions underlying the experienced conformational transitions, quantum chemical calculations were performed. All theoretical computations were conducted using the Gaussian 09 (G09) software package [1]. Graphical representation of the structures were created using Pymol (The PyMol Molecular Graphics System, DeLano Scientific, Palo Alto, CA). To investigate interaction of CM15 in helical conformation with the studied negatively charged compounds, initial models were built as follows. Helical starting structure of CM15 was taken from an NMR experiment.[2] All drug and dye molecules (suramin, pamoic acid, cromolyn, Congo red, trypan blue) were built using their solution phase, deprotonated forms, where the sulfonate and carboxylate groups consequently possess a negative charge. Initial structures of these compounds were optimized at the semi-empirical level, using the PM3MM method. PM3MM was developed from PM3 to include molecular mechanics correction for amide linkage present in peptides.[3] The semi-empirical approach was chosen as it provides fast and efficient insight into the molecular level interactions with reasonable accuracy, without the cumbersome parametrization procedure required for in depth molecular dynamics simulations, a study beyond our current focus. Furthermore, the small molecule-peptide complexes are large molecular systems, up to 405 atoms, consequently preventing efficient use of higher quantum chemical methods, such as ab initio or density functional theory techniques.

All complexes were optimized starting from 3 different relative positions of the CM15 helix and the addressed negatively charged compound, requiring a total of 15 different calculations. These all resulted in optimized structures except two positions for suramin and one for trypan blue complexes. The latter ones were subject of several optimization attempts, but failed to reach full convergence. Presented structures were chosen from the pool of three different binding modes based on their relative energies as well as on the quantity and quality of the intermolecular salt-bridges, hydrogen bonds, and stacking interactions.

Protein Name	Disordered Sequence	DisProt ID
Eukaryotic peptide chain release factor subunit 1 (*H. sapiens*)	$_{423}$EYQGGDDEFFDLDDY$_{434}$	DP00310
Ribonucleoside-diphosphate reductase M2 subunit (*M.musculus*)	$_{353}$NISLEGKTNFFEKRVGEYQ RMGVMSNSTENSFTLDADF$_{3}$ $_{83}$	DP00462
DnaK suppressor protein (*E. coli*)	$_{17}$IAGVEPYQEKPGEEYMN$_{33}$	DP00414
IIβ Phosphatidylinositol phosphate kinase (*H. sapiens*)	$_{220}$STVAREASDKEKAKDLPT FKDNDFLNEGQKL$_{250}$	DP00054
Thymidylate synthase (*H. sapiens*)	$_{107}$KIWDANGSRDFLDSLGFS TREE$_{128}$	DP00073
DNA topoisomerase 1 (*H. sapiens*)	$_{175}$KPKNKDKDKKVPEPDNK KKKPKKEEEQKWKWWEEE RYPEG$_{214}$	DP00075
SHC-transforming protein 1 (*H. sapiens*)	$_{127}$GQLGGEEWTRHGSFVNKP TRGWLHP$_{149}$	DP00154
Cyclin-H (*H. sapiens*)	$_{288}$NVITKKRKGYEDDDYVSK KSKHEEEEWTDDDLVESL$_{323}$	DP00307
Cbp/p300-interacting transactivator 2 (*H. sapiens*)	$_{220}$TDFIDEEVLMSLVIEMGLD RIKELPELWLGQNEFDFMTD FVCKQQPSRVS$_{269}$	DP00356
Histo-blood group ABO system transferase (*H. sapiens*)	$_{179}$KRWQDVSMRRMEMISD$_{194}$	DP00339
Alcohol sulfotransferase (*H. sapiens*)	$_{13}$WDTYEDDISEISQK$_{26}$	DP00404
Ras-related protein Ral-A (*H. sapiens*)	$_{72}$QEDYAAIRDNYF$_{83}$	DP00581
60S acidic ribosomal protein P2 (*H. sapiens*)	$_{102}$SEESDDDMGFGLFD$_{115}$	DP00793
Small heat shock protein HSP16.5 (*M. jannaschii*)	$_{1}$MFGRDPFDSLFERMFKEFF ATPMTGTTMIQSS$_{32}$	DP00067
DNA gyrase inhibitor YacG (*E. coli*)	$_{40}$WAAEEKRIPSSGDLSESDD WSEEPKQ$_{65}$	DP00202
Calcyclin-binding protein (*M.musculus*)	$_{178}$EKPSYDTEADPSEGLMNV LKKIYEDGDDDMKRTINKA WVESREKQAREDTEF$_{229}$	DP00226

Supplementary Table 1

Selected examples for experimentally verified, CM15-like disordered sequences consisting of charged (red) as well as aromatic residues (bold). Data were obtained from the DisProt database at http://www.disprot.org/.

Target protein	Length (a.a.)	Disorder (%)	UniProt ID	Refs.
Protamine 1B (*Rainbow trout*)	33	100	P02326	[4]
Basic fibroblast growth factor (*H. sapiens*)	288	55.56	P09038	[5]
Insulin-like growth factor 1 (*H. sapiens*)	195	51.28	P05019	[5]
N-lysine methyltransferase KMT5A (*H. sapiens*)	393	49.87	Q9NQR1	[6]
NAD^+-dependent protein deacetylase sirtuin-1 (*H. sapiens*)	747	47.93	Q96EB6	[7]
Histone-lysine *N*-methyltransferase EHMT1 (*H. sapiens*)	1298	43.61	Q9H9B1	[6]
M-phase inducer phosphatase 1 (*H. sapiens*)	524	39.89	P30304	[8]
Interleukin-2 receptor α-subunit (*H. sapiens*)	272	38.97	P01589	[9]
Platelet-derived growth factor subunit B (*H. sapiens*)	241	33.20	P01127	[5]
Hepatitis B virus core protein	185	32.43	G9BNJ2	[4]
Tyrosine-protein phosphatase non-receptor type 1 (*H. sapiens*)	435	27.82	P18031	[8]
Tyrosyl-DNA phosphodiesterase 1 (*H. sapiens*)	608	27.47	Q9NUW8	[10]
D_2 dopamine receptor (*H. sapiens*)	443	27.31	P14416	[11]
Receptor-type tyrosine-protein phosphatase C (*H. sapiens*)	1304	27.07	P08575	[8]
Tyrosine-protein phosphatase YopH (*Y. enterocolitica*)	468	25.43	P15273	[8,12]
DNA topoisomerase 2 (*S. cerevisiae*)	1428	25.00	P06786	[13]
Carcinoembryonic antigen-related cell adhesion molecule 1 (*H. sapiens*)	526	24.52	P13688	[14]
P_{2X2} purinoceptor (*R. norvegicus*)	472	22.25	P49653	[15,16]
Receptor-type tyrosine-protein phosphatase α (*H. sapiens*)	802	20.82	P18433	[8]

Target protein	Length (a.a.)	Disorder (%)	UniProt ID	Refs.
P_{2Y2} purinoceptor (*H. sapiens*)	377	20.16	P41231	[17,18]
NAD^+-dependent protein deacetylase sirtuin-1 (*H. sapiens*)	389	20.05	Q8IXJ6	[7]
Protein kinase C type β (*R. norvegicus*)	671	18.93	P68403	[19]
Tumor necrosis factor-α (*H. sapiens*)	233	18.88	P01375	[20]
DNA polymerase α catalytic subunit (*H. sapiens*)	1462	18.67	P09884	[21]
Heat shock protein 104 (*S. cerevisiae*)	908	16.52	P31539	[22]
P_{2X1} purinoceptor (*R. norvegicus*)	399	12.78	P47824	[15,17,23]
Epidermal growth factor receptor (*H. sapiens*)	1210	12.40	P00533	[24]
Dual specificity protein phosphatase 3 (*H. sapiens*)	185	11.89	P51452	[12]
Nuclear receptor subfamily 1 group I member 2 (*H. sapiens*)	434	11.29	O75469	[25]
Complement control protein C3 (*Vaccinia virus*)	263	9.51	P68638	[26]

Supplementary Table 2

Disorder prediction results for various proteins found experimentally to be affected by suramin. The percentage of residues involved in predicted disordered regions of proteins is based on the corresponding MobiDB consensus score (http://mobidb.bio.unipd.it).[27]

Target protein	Length (a.a.)	Disorder (%)	UniProt ID	Refs.
Microtubule-associated protein tau (*H. sapiens*)	758	89.45	P10636	[28,29]
α-Synuclein (*H. sapiens*)	140	41.43	P37840	[30]
Eukaryotic peptide chain release factor GTP-binding subunit (*S. cerevisiae*)	685	38.10	P05453	[31,32]
Choline *O*-acetyltransferase (*H. sapiens*)	748	20.59	P28329	[33]
Dihydrofolate reductase type 2 (*E. coli*)	78	20.51	P00383	[34]
PH domain leucine-rich repeat-containing protein phosphatase 2 (*H. sapiens*)	1323	17.54	Q6ZVD8	[35]
RecA (*E. coli*)	353	9.63	P0A7G6	[36]

Supplementary Table 3

Disorder prediction results for various proteins found experimentally to be affected by Congo red. The percentage of residues involved in predicted disordered regions of proteins is based on the corresponding MobiDB consensus score (http://mobidb.bio.unipd.it).[27]

Target protein	Length (a.a.)	Disorder (%)	UniProt ID	Refs.
Tyrosine-protein phosphatase non-receptor type 1 (*H. sapiens*)	435	27.82	P18031	[37]
β-Arrestin-2 (*H. sapiens*)	409	19.07	P32121	[38]
Receptor-type tyrosine-protein phosphatase F (*H. sapiens*)	1907	15.57	P10586	[37]
DNA polymerase β (*H. sapiens*)	335	9.85	P06746	[39]
G-protein coupled receptor 35 (*H. sapiens*)	309	9.06	Q9HC97	[38,40,41]

Supplementary Table 4

Disorder prediction results for various proteins found experimentally to be affected by pamoic acid. The percentage of residues involved in predicted disordered regions of proteins is based on the corresponding MobiDB consensus score (http://mobidb.bio.unipd.it/).[27]

Target protein	Length (a.a.)	Disorder (%)	UniProt ID	Refs.
β-Arrestin-2 (*H. sapiens*)	409	19.07	P32121	[42]
Protein S100-A13 (*H. sapiens*)	98	18.37	Q99584	[43]
Protein S100-B (*Bos taurus*)	92	17.39	P02638	[43]
Protein S100-A13 (*Bos taurus*)	98	13.27	P79342	[44]
Protein S100-A12 (*Bos taurus*)	92	10.87	P79105	[44]
G-protein coupled receptor 35 (*H. sapiens*)	309	9.06	Q9HC97	[41,45]

Supplementary Table 5

Disorder prediction results for various proteins found experimentally to be affected by cromolyn. The percentage of residues involved in predicted disordered regions of proteins is based on the corresponding MobiDB consensus score (http://mobidb.bio.unipd.it/).[27]

Ligand:CM15 molar ratio	Heparin		Suramin		Congo red		Pamoic acid	
	D_h	P.d.	D_h	P.d.	D_h	P.d.	D_h	P.d.
1:2	–	–	–	–	–	–	–	–
1:1	850 (±382)	45	1098 (±569)	52	799 (±441)	55	–	–
2:1	1902 (±1416)	75	859 (±647)	75	1460 (±1033)	71	131 (±76)	58
3:1	870 (±426)	49	1053 (±589)	57	1577 (±968)	61	370 (±188)	51
4:1	1021 (±519)	51	1453 (±1016)	70	937 (±478)	51	335 (±261)	78
5:1	819 (±436)	53	1477 (±532)	36	880 (±289)	33	427 (±282)	66

Supplementary Table 6

Polydispersity (P.d. in %) of ligand-CM15 samples and mean hydrodynamic diameter (D_h in nm) of the particles measured by DLS method.

Ligand	Intermol. Salt bridges		Intermol. H-bonds		Intermol. π-interaction	
	No.[a]	Residue	No.	Residues	Residue	Type
Trypan blue	5	Lys3, Lys6, Lys7, Lys13	-	-	Trp2	Stacking, T-shaped
Suramin	8	Lys1, Lys3, Lys6, Lys7, Lys13	1	Lys6	Phe5	Stacking, T-shaped
Congo red	3	Lys1, Lys6, Lys13,	-	-	Phe5	Stacking, T-shaped
Pamoic acid	2	Lys1, Lys13,	-	-	Lys6	Cation-π
Cromolyn	2	Lys1, Lys13,	2	Lys6	Trp2	Stacking, Edge-edge

[a]: Number of interactions found.

Supplementary Table 7

Assigned intermolecular interactions for the lowest energy complexes of the investigated small molecule-CM15 systems.

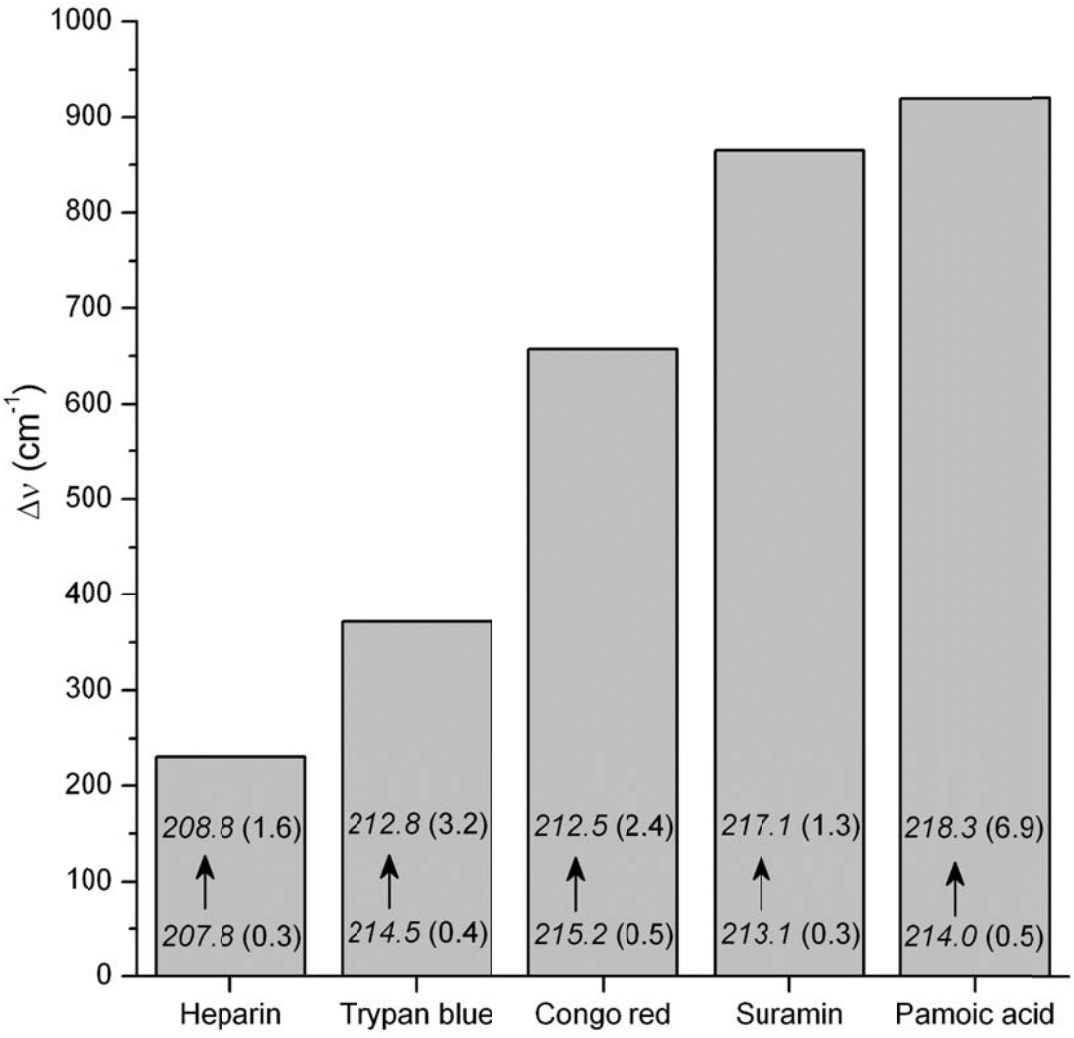

Supplementary Figure 1

Spectral shift of the isodichroic points of the CD spectra during the titration of CM15 with heparin and organic small molecules. Isodichroic points are the zero crossover positions of CD curves of ligand-free and ligand-loaded forms of the peptide. The 'Y' axis denotes the differences (in wavenumber) between wavelength values (nm) shown inside the columns. Arrows indicate the wavelength shift of the isodichroic point upon increase the ligand/peptide molar ratio (in parentheses).

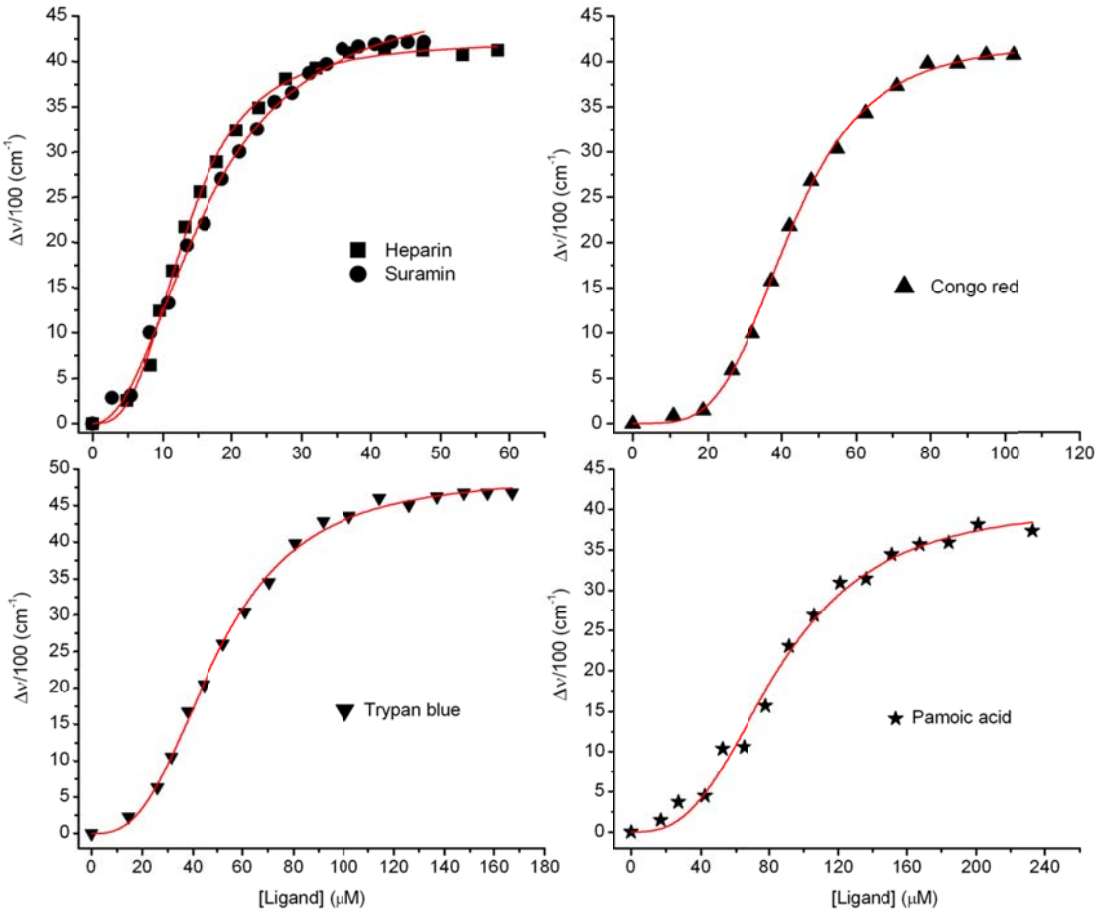

Supplementary Figure 2

CD titration data of CM15 plotted against the ligand concentration in the sample solutions. Δν: the shift in wavenumber of the zero cross-over point measured during the titrations (see text for more details). Solid lines are the results of non-linear curve fitting analysis performed by using the "One site - specific binding with Hill slope" equation built in the GraphPad Prism software (ver. 6.01, San Diego, California, USA).

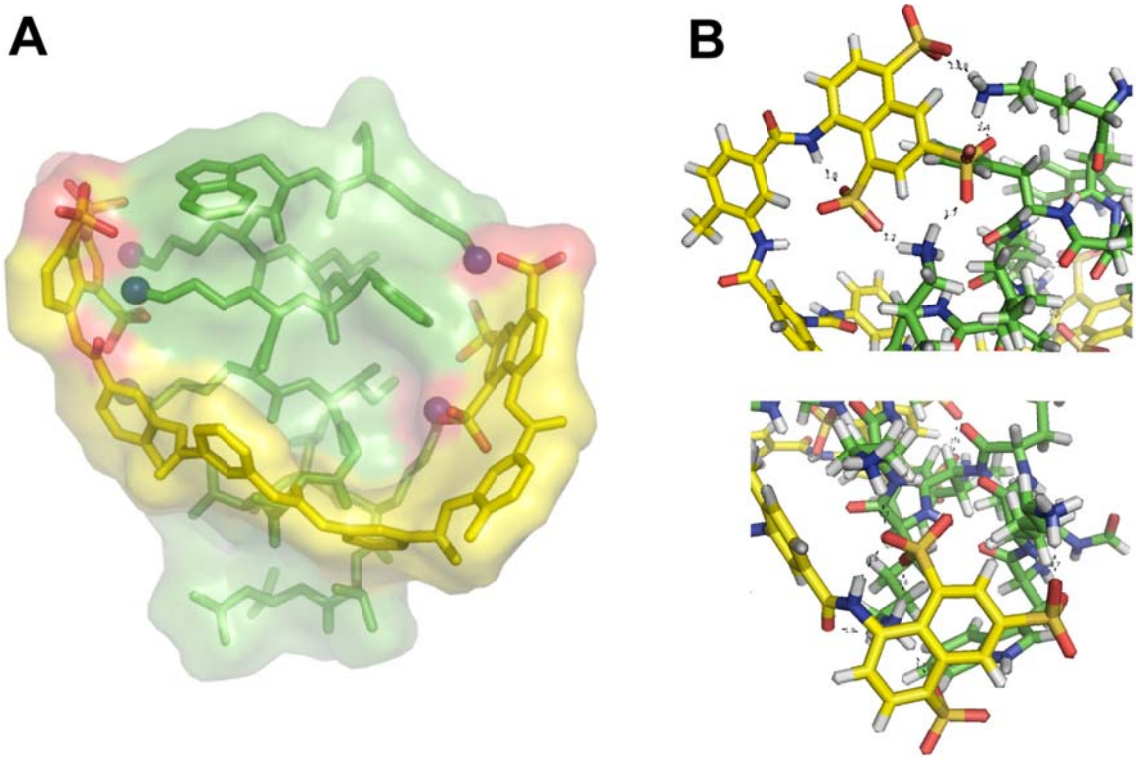

Supplementary Figure 3

Structure of the suramin-CM15 complex optimized using the PM3MM method. **A**: Surface model of the complex where the peptide and the suramin molecule are shown as green and yellow sticks, respectively. Oxygen atoms on suramin are highlighted by red, the nitrogens on the lysine side chains are marked as blue spheres. **B**: Structural details of the H-bond network formed between suramin (yellow sticks) and CM15 lysines (green sticks). H-bonds are marked by dashed lines, with atom-atom distances displayed in Ångströms.

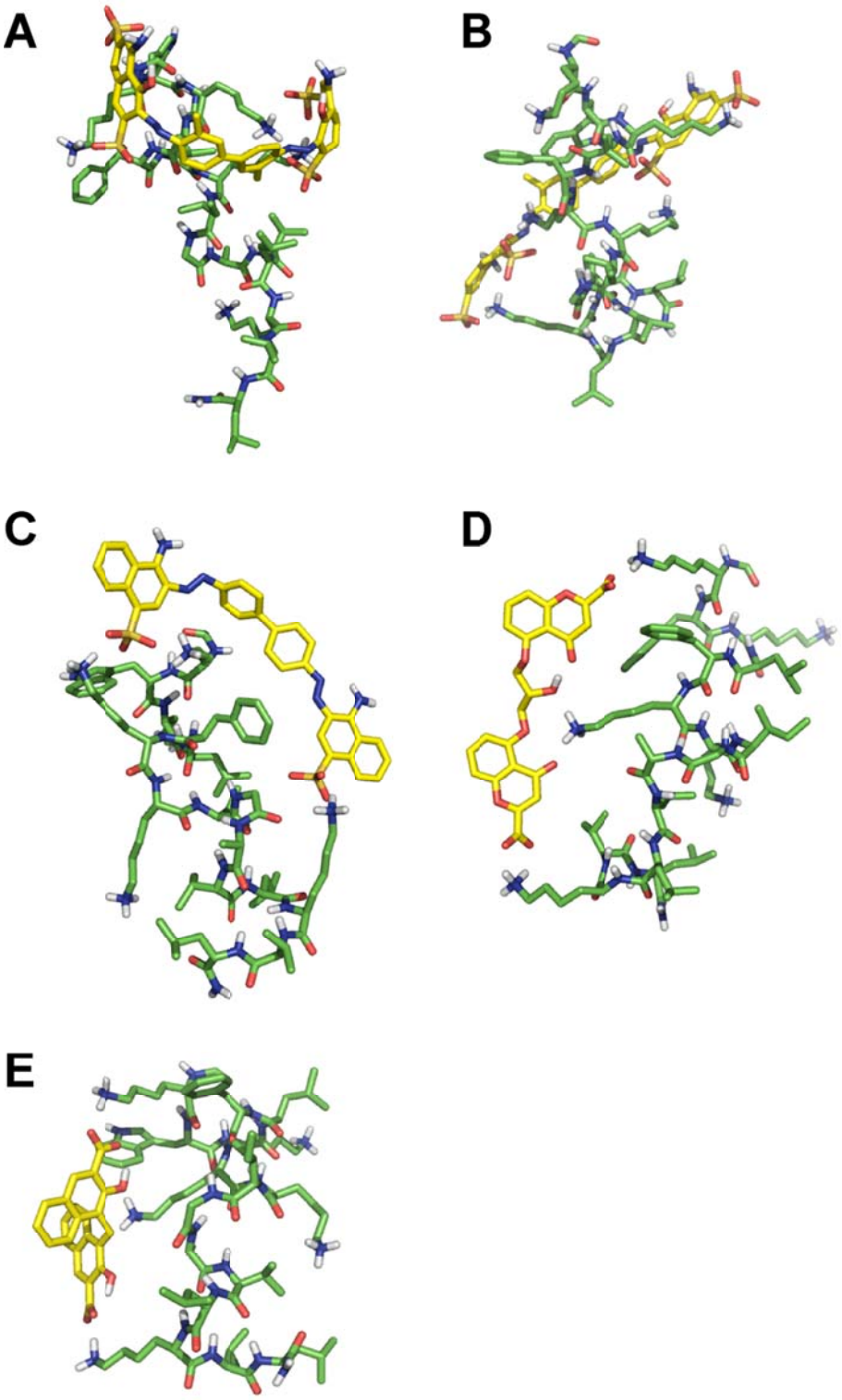
A
B
C
D
E

Supplementary Figure 4

Structures of the small molecule-CM15 complexes obtained at the PM3MM level of theory. For all models the organic small molecules are represented by yellow sticks, whereas the CM15 molecules are as green sticks. The models are oriented with the N-terminal residue of CM15 located at the top of each panel. **A, B**: Two configurations of the trypan blue-CM15 complex. **A:** The one which does not involve H-bonds between the ligand and lysine residues from both terminals (*i.e.* Lys13 in this particular case) cannot induce folding of the entire CM15 sequence, and thus the calculation optimized into a partially unfolded conformation. **C**: The most stable complex of Congo red and CM15. **D**: The most stable complex of cromolyn and CM15. **E**: The most stable complex of pamoic acid and CM15.

References

1. M. J. Frisch, G. W. Trucks, H. B. Schlegel, G. E. Scuseria, M. A. Robb, J. R. Cheeseman, G. Scalmani, V. Barone, B. Mennucci, G. A. Petersson, H. Nakatsuji, M. Caricato, X. Li, H. P. Hratchian, A. F. Izmaylov, J. Bloino, G. Zheng, J. L. Sonnenberg, M. Hada, M. Ehara, K. Toyota, R. Fukuda, J. Hasegawa, M. Ishida, T. Nakajima, Y. Honda, O. Kitao, H. Nakai, T. Vreven, J. A. Montgomery Jr., J. E. Peralta, F. Ogliaro, M. J. Bearpark, J. Heyd, E. N. Brothers, K. N. Kudin, V. N. Staroverov, R. Kobayashi, J. Normand, K. Raghavachari, A. P. Rendell, J. C. Burant, S. S. Iyengar, J. Tomasi, M. Cossi, N. Rega, N. J. Millam, M. Klene, J. E. Knox, J. B. Cross, V. Bakken, C. Adamo, J. Jaramillo, R. Gomperts, R. E. Stratmann, O. Yazyev, A. J. Austin, R. Cammi, C. Pomelli, J. W. Ochterski, R. L. Martin, K. Morokuma, V. G. Zakrzewski, G. A. Voth, P. Salvador, J. J. Dannenberg, S. Dapprich, A. D. Daniels, Ö. Farkas, J. B. Foresman, J. V. Ortiz, J. Cioslowski and D. J. Fox, *Gaussian 03, Revision C.02*, Gaussian, Inc., Wallingford, CT, USA, 2004.

2. M. Respondek, T. Madl, C. Gobl, R. Golser and K. Zangger, *J. Am. Chem. Soc.*, 2007, **129**, 5228-5234.

3. J. J. P. Stewart, *J. Comput. Chem.*, 1989, **10**, 221-264.

4. M. Okabe, M. Enomoto, H. Maeda, K. Kuroki and K. Ohtsuki, *Biol. Pharm. Bull.*, 2006, **29**, 1810-1814.

5. C. R. Middaugh, H. Mach, C. J. Burke, D. B. Volkin, J. M. Dabora, P. K. Tsai, M. W. Bruner, J. A. Ryan and K. E. Marfia, *Biochemistry*, 1992, **31**, 9016-9024.

6. G. Ibanez, D. Shum, G. Blum, B. Bhinder, C. Radu, C. Antczak, M. Luo and H. Djaballah, *Comb. Chem. High Throughput Screen.*, 2012, **15**, 359-371.

7. J. Trapp, R. Meier, D. Hongwiset, M. U. Kassack, W. Sippl and M. Jung, *ChemMedChem*, 2007, **2**, 1419-1431.

8. D. F. McCain, L. Wu, P. Nickel, M. U. Kassack, A. Kreimeyer, A. Gagliardi, D. C. Collins and Z. Y. Zhang, *J. Biol. Chem.*, 2004, **279**, 14713-14725.

9. G. B. Mills, N. Zhang, C. May, M. Hill and A. Chung, *Cancer Res.*, 1990, **50**, 3036-3042.

10. S. Walker, C. Meisenberg, R. A. Bibby, T. Askwith, G. Williams, F. H. Rininsland, L. H. Pearl, A. W. Oliver, S. El-Khamisy, S. Ward and J. R. Atack, *Anal. Biochem.*, 2014, **454**, 17-22.

11. M. Waldhoer, E. Bofill-Cardona, G. Milligan, M. Freissmuth and C. Nanoff, *Mol. Pharmacol.*, 1998, **53**, 808-818.

12. Y. L. Zhang, Y. F. Keng, Y. Zhao, L. Wu and Z. Y. Zhang, *J. Biol. Chem.*, 1998, **273**, 12281-12287.

13. K. Bojanowski, S. Lelievre, J. Markovits, J. Couprie, A. Jacquemin-Sablon and A. K. Larsen, *Proc. Natl. Acad. Sci. USA*, 1992, **89**, 3025-3029.

14. M. W. Beukers, C. J. Kerkhof, M. A. van Rhee, U. Ardanuy, C. Gurgel, H. Widjaja, P. Nickel, I. J. AP and W. Soudijn, *Naunyn Schmiedebergs Arch. Pharmacol.*, 1995, **351**, 523-528.

15. A. D. Michel, K. Lundstrom, G. N. Buell, A. Surprenant, S. Valera and P. P. Humphrey, *Br. J. Pharmacol.*, 1996, **118**, 1806-1812.

16. C. Wolf, C. Rosefort, G. Fallah, M. U. Kassack, A. Hamacher, M. Bodnar, H. Wang, P. Illes, A. Kless, G. Bahrenberg, G. Schmalzing and R. Hausmann, *Mol. Pharmacol.*, 2011, **79**, 649-661.

17. M. U. Kassack, K. Braun, M. Ganso, H. Ullmann, P. Nickel, B. Boing, G. Muller and G. Lambrecht, *Eur. J. Med. Chem.*, 2004, **39**, 345-357.

18. C. E. Müller, *Curr. Pharm. Des.*, 2002, **8**, 2353-2369.

19. Z. Khaled, D. Rideout, K. R. O'Driscoll, D. Petrylak, A. Cacace, R. Patel, L. C. Chiang, S. Rotenberg and C. A. Stein, *Clin. Cancer Res.*, 1995, **1**, 113-122.

20. F. Mancini, C. M. Toro, M. Mabilia, M. Giannangeli, M. Pinza and C. Milanese, *Biochem. Pharmacol.*, 1999, **58**, 851-859.

21. H. K. Jindal, C. W. Anderson, R. G. Davis and J. K. Vishwanatha, *Cancer Res.*, 1990, **50**, 7754-7757.

22. M. P. Torrente, L. M. Castellano and J. Shorter, *PLoS One*, 2014, **9**, e110115.

23. G. Lambrecht, K. Braun, M. Damer, M. Ganso, C. Hildebrandt, H. Ullmann, M. U. Kassack and P. Nickel, *Curr. Pharm. Des.*, 2002, **8**, 2371-2399.

24. P. M. Fischer and D. P. Lane, *Curr. Med. Chem.*, 2000, **7**, 1213-1245.

25. S. J. Shukla, S. Sakamuru, R. Huang, T. A. Moeller, P. Shinn, D. Vanleer, D. S. Auld, C. P. Austin and M. Xia, *Drug Metab. Dispos.*, 2011, **39**, 151-159.

26. V. K. Ganesh, S. K. Muthuvel, S. A. Smith, G. J. Kotwal and K. H. M. Murthy, *Biochemistry*, 2005, **44**, 10757-10765.

27. E. Potenza, T. Di Domenico, I. Walsh and S. C. Tosatto, *Nucleic Acids Res.*, 2015, **43**, D315-320.

28. K. I. Lira-De Leon, P. Garcia-Gutierrez, I. N. Serratos, M. Palomera-Cardenas, P. Figueroa-Corona Mdel, V. Campos-Pena and M. A. Meraz-Rios, *J. Alzheimers Dis.*, 2013, **35**, 319-334.

29. E. Chang, N. S. Honson, B. Bandyopadhyay, K. E. Funk, J. R. Jensen, S. Kim, S. Naphade and J. Kuret, *Curr. Alzheimer Res.*, 2009, **6**, 409-414.

30. A. S. Maltsev, A. Grishaev and A. Bax, *Biochemistry*, 2012, **51**, 631-642.

31. J. R. Glover, A. S. Kowal, E. C. Schirmer, M. M. Patino, J. J. Liu and S. Lindquist, *Cell*, 1997, **89**, 811-819.

32. B. Y. Feng, B. H. Toyama, H. Wille, D. W. Colby, S. R. Collins, B. C. May, S. B. Prusiner, J. Weissman and B. K. Shoichet, *Nat. Chem. Biol.*, 2008, **4**, 197-199.

33. H. G. Mautner, R. E. Merrill, S. F. Currier and G. Harvey, *J. Med. Chem.*, 1981, **24**, 1534-1537.

34. D. Bastien, M. C. Ebert, D. Forge, J. Toulouse, N. Kadnikova, F. Perron, A. Mayence, T. L. Huang, J. J. Vanden Eynde and J. N. Pelletier, *J. Med. Chem.*, 2012, **55**, 3182-3192.

35. E. Sierecki, W. Sinko, J. A. McCammon and A. C. Newton, *J. Med. Chem.*, 2010, **53**, 6899-6911.

36. T. J. Wigle and S. F. Singleton, *Bioorg. Med. Chem. Lett.*, 2007, **17**, 3249-3253.

37. S. Shrestha, Y. S. Shim, K. C. Kim, K. H. Lee and H. Cho, *Bioorg. Med. Chem. Lett.*, 2004, **14**, 1923-1926.

38. L. Jenkins, N. Harries, J. E. Lappin, A. E. MacKenzie, Z. Neetoo-Isseljee, C. Southern, E. G. McIver, S. A. Nicklin, D. L. Taylor and G. Milligan, *J. Pharmacol. Exp. Ther.*, 2012, **343**, 683-695.

39. H.-Y. Hu, J. K. Horton, M. R. Gryk, R. Prasad, J. M. Naron, D.-A. Sun, S. M. Hecht, S. H. Wilson and G. P. Mullen, *J. Biol. Chem.*, 2004, **279**, 39736-39744.

40. L. Jenkins, J. Brea, N. J. Smith, B. D. Hudson, G. Reilly, N. J. Bryant, M. Castro, M. I. Loza and G. Milligan, *Biochem. J.*, 2010, **432**, 451-459.

41. M. Funke, D. Thimm, A. C. Schiedel and C. E. Muller, *J. Med. Chem.*, 2013, **56**, 5182-5197.

42. A. E. MacKenzie, G. Caltabiano, T. C. Kent, L. Jenkins, J. E. McCallum, B. D. Hudson, S. A. Nicklin, L. Fawcett, R. Markwick, S. J. Charlton and G. Milligan, *Mol. Pharmacol.*, 2014, **85**, 91-104.

43. Y. Arendt, A. Bhaumik, R. Del Conte, C. Luchinat, M. Mori and M. Porcu, *ChemMedChem*, 2007, **2**, 1648-1654.

44. T. Shishibori, Y. Oyama, O. Matsushita, K. Yamashita, H. Furuichi, A. Okabe, H. Maeta, Y. Hata and R. Kobayashi, *Biochem. J.*, 1999, **338 (Pt 3)**, 583-589.

45. D. Thimm, M. Funke, A. Meyer and C. E. Muller, *J. Med. Chem.*, 2013, **56**, 7084-7099.